Wall shear rate components for wavy Taylor-Couette flow

Magdalena Kristiawan, Tomáš Jirout, Alioune El Faye, Vaclav Sobolik

HAL Id: hal-02756409

https://hal.inrae.fr/hal-02756409

Submitted on 3 Jun 2020

C9. CHISA 2010, full text

Wall shear rate components for wavy Taylor-Couette flow

Magdalena Kristiawan[1], Tomas Jirout[2], Alioune El Faye[1] and Vaclav Sobolík [1]*
[1]University of La Rochelle, UFR Sciences, LEPTIAB
[2]Czech Technical University, Faculty of Mechanical Engineering, Prague
vsobolik@univ-lr.fr. Av. Michel Crepeau, La Rochelle, 17042, France

Experiments were carried out in the wavy flow between concentric cylinders with the inner cylinder rotating and outer cylinder fixed. The radius and aspect ratios were 0.8 and 44, respectively. The electrodiffusion method with a three-segment and simple micro-electrodes was used for study of the axial and azimuthal components of shear rate at the outer cylinder. The axial distributions of these components were obtained by sweeping the vortices along the probes using a slow axial flow. The wavelength and phase celerity of waves, height of vortices and their drifting velocity were calculated from the measured limiting diffusion currents.

1. Introduction

Several techniques can be used for the measurements of shear rates at the solid-liquid interface. The measurement of the current of an electrochemical reaction, i.e. the electrodiffusion (polarographic) method (Cognet 1971, Lebouché 1970), is the only method able to follow the space distribution and time evolution of wall shear rates. This method is based on the measurement of the electric current limited by the transfert of actives species to the working electrode. Using a redox reaction, repetitive measurements can be carried out with a system which does not require addition of active compounds as in the case of the above mentioned method. The measurements are confined to the diffusion boundary layer which is very thin (several micrometers) in the electrolyte solutions (high Schmidt number). This fact distinguishes the electrodiffusion method from the other methods like laser Doppler anemometry, hot film anemometry and particle image velocimetry.

The three-segment probes (see Fig. 1) are composed of three insulated circular sectors that act as working electrodes (Sobolik et al. 1988). For the evaluation of flow direction, we make use of the non-linear dependence of the limiting current density on the distance from the forward electrode edge, $i(x) \sim x^{-1/3}$ (Lévêque 1928). The forward sector has higher current than the sector that lies in his shade. Hence, shear rate and its components can be calculated from the limiting diffusion currents passing through the three segments (Wein and Sobolik 1987).

In this work, the electrodiffusion method with a three-segment and simple micro-electrodes was used for the study of the axial (γ_z) and azimuthal (γ_θ) components of shear rate at the outer wall of Taylor-Couette flow.

2. Experimental

Experiments were carried out in the flow between concentric cylinders with the inner cylinder rotating and outer cylinder fixed. The inner cylinder was driven by a stepper motor with electronically controlled rotation rate. The diameters of the outer and inner cylinders were equal to 62 and 49.6 mm, respectively. This corresponds to the radius ratio, R1/R2 = 0.8. The aspect ratio was about 44. For simultaneous observation of flow pattern and measurement of shear rate and vortex characteristics a Kalliroscope solution was added to the electrolyte.

The flow regime with wavy Taylor vortices, i.e. vortices with steady azimuthal waves was studied. The vortices were swept past the electrodes by a slow axial flow. Using three-segment probe, see Fig. 1, complete maps of axial and azimuthal components of shear rate and their fluctuations at the wall of the outer cylinder were obtained as a function of axial co-ordinate and time. The vortex size (height) and the number and celerity of azimuthal waves were measured by an array of simple electrodes mounted in the wall of the outer cylinder. The arrangement of the electrodiffusion probes along the perimeter of the outer cylinder is shown in Fig. 2. The azimuthal (γ_θ) and axial (γ_z) components of the shear rate (γ) were measured by the three-segment probe 3s with a diameter of 0.5 mm. Simple probes e4, e5 and e6 were formed by circular electrodes with the same diameter (0.5 mm). The celerity of azimuthal waves was calculated from the time lag (correlation) of currents delivered by e4 and e5. The wave period was obtained from autocorrelation of the current through the electrode e4. The wavelength was calculated from wave period and celerity. The vortices were driven by a slow axial flow (z-direction) along the probes. The drifting vortex velocity was calculated from the time necessary for a vortex to cover the distance between e5 and e6. The height of vortices was obtained from their period and drifting velocity. The correlations and fast Fourier transformation of measured currents were calculated using Scilab software
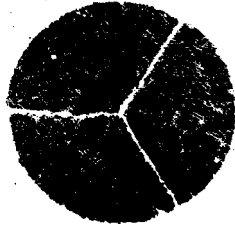

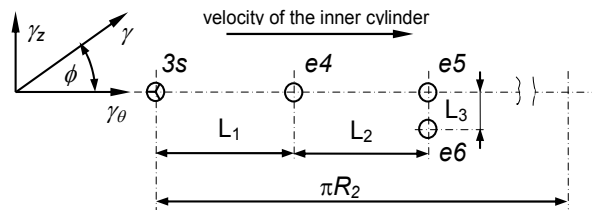Fig. 1. Three-segment probe with a diameter of 0.5 mm.

Fig. 2. Arrangement of the three-segment probe 3s and simple electrodes e4, e5 and e6 along the perimeter.

3. Results and discussion

The limiting diffusion current histories measured by the three-segment probe (I1, I2, I3) and three simple probes (I4, I5, I6) at Ta=323 are shown in Fig. 3. The measurements were taken over about one and half vortex pairs with a sampling frequency of 40 1/s. The vortex drifting velocity was 0.14 mm/s. Knowing the drifting velocity, the time axis
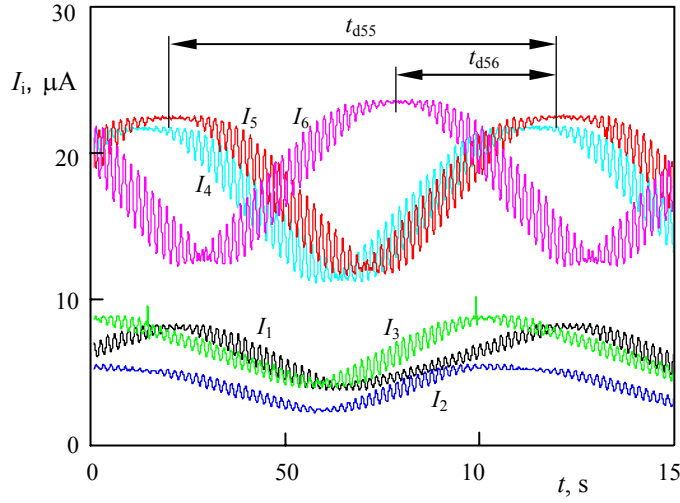
Fig. 3. Current histories: I1, I2, I3 – three-segment
probe; I4, I5, I6 – simple electrodes; Ta =323

can be transformed to the axial coordinate z. The time td55 corresponds to the passage of a vortex pair along the probe e5 in axial direction, whereas the time td56 indicates the passage of vortex crest between the probes e5 and e6. The time td56 was used for calculation of vortex drifting velocity and td55 for calculation of vortex height. The azimuthal waves manifest themselves in the signal oscillations. These waves were studied by means of the current correlations R4i, calculated with respect to I4. The time lag tw45 between the autocorrelation of R44 and correlation R45 (see Fig. 4) corresponds to the passage of a selected wave point between e4 and e5, and tw44 to the passage of one wave past e4. The time tw45 was used for the calculation of azimuthal wave celerity and the wave period tw44 for calculation of wavelength. The number of
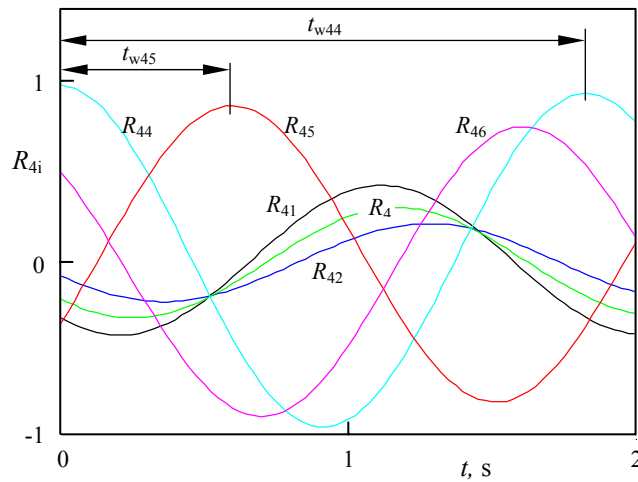
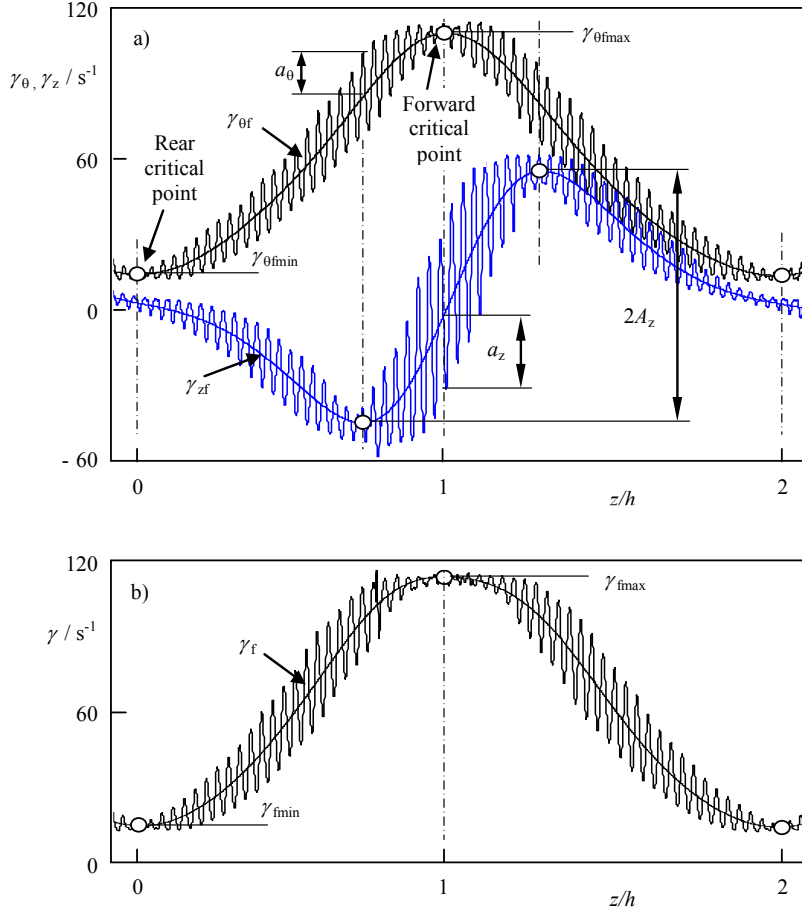

Fig. 4. Correlations with respect to the current I4

3

Fig. 5. Characteristic values of wall shear rate (b) and its components (a) at Ta = 320.

azimuthal waves was obtained by dividing the perimeter of the outer cylinder by the wavelength. The shear rate components calculated from currents I1, I2, I3 are shown in Fig. 5a. The z-coordinate concerns the height of vortices but it is irrelevant for the wavelength of azimuthal waves. The period of azimuthal waves shown in Fig. 5a is a function of number of waves, angular velocity of waves and drifting velocity of vortices. The amplitude of the shear rate components at different position z is given by the envelope of the oscillations which is not shown. The meaning of different symbols is also shown in this figure. The notion of filtered shear rate is introduced. This means the shear rate or its components from which the azimuthal waves were filtred out by a Butterworth filter, see $\gamma_{\theta f}$ and γ_{zf} in Fig. 5a. The course of filtered wall shear rates and their components is similar to the wall shear rates in Taylor-Couette non wavy flow (Sobolik et al.).

From the point of view of the axial velocity, the outflow creates a forward critical point on the outer cylinder, see Fig. 5a. The azimuthal component of shear rate exhibits a maximum at this point and a minimum at the rear critical point (inflow). The axial component of shear rate is zero at these points. In fact, there is a small finite value of

4

axial shear rate due to the drifting velocity of vortices. The amplitude of azimuthal waves, given by the envelope of oscillations, has azimuthal a_θ, and axial component a_z. The azimuthal component is zero in forward and rear critical points. The axial component has a maximum in forward critical point and it is very small at the extremes of γ_{zf}. Like in the classical forward critical point, the amplitude of axial oscillations, a_z, exhibits maxima and the variation of γ_{zf} is steep and almost linear. It is much steeper than in the inflow. The outflow has the form of a narrow jet with a high radial and azimuthal velocity.

Even if the amplitude of the axial component of shear rate has its maximum at the forward critical point, the oscillations of absolute value shear rate are very small, see Fig. 5b. It is due to the high value of azimuthal shear rate which is steady at this point.

We observed the transition from Taylor vortex flow into wavy vortex flow at Ta= 80.5. This value is much higher than the values calculated by Jones 1985. From his Fig. 3, we deducted values of 55.0, 57.6 and 64.5 for set-up of 1, 2 and 3 waves, respectively. We found always three waves at the transition which is in agreement with the simulations carried out by Jones.

The components of wall shear rate were measured at different rotational rate (Ta=97, 202 and 483). At the lowest rotational rate the regime of three azimuthal waves was stable. The characteristic values of the vortices are shown in Table 1.

Tab. 1: Parameters of wavy vortex flow.

Ta	n	A_z	a_z	a_θ	$\gamma_{\theta\,max}$	$h.10^3$
97	3	4.8	4.1	2.4	13.7	11.2
202	4	21.1	14.3	7.5	46.3	11.1
483	2	60.4	74.4	52.9	194	11.1

The axial component of the wall shear rate can be compared to the wall shear rate in classical impinging jet even if the azimuthal component in the forward stagnation point exhibits a maximum. According to Prandtl's boundary theory (Schlichting 1968), it holds for the stagnation region of an impinging jet that the wall shear rate is proportional to the distance from the stagnation point. The maximum of the wall shear rate is at the transition from the stagnation zone to the wall jet region. The spatial distribution of the wall shear rate fluctuations depends on the jet Reynolds number and the distance of the orifice from the plate (Alekseenko and Markowich 1994). It can have a maximum or minimum in the stagnation point or a constant value in the jet region. At Ta=97, the amplitude of γ_z had maximum at the forward stagnation point and with increasing Ta the amplitude became almost constant in the outflow zone. Jones (1985) concluded that the strong azimuthal jets at the outflow region destabilize the flow making the vortices wavy. Coughlin and Marcus (1992) supposed that the both radial and azimuthal jets and axial gradient of the azimuthal velocity are responsible for the waviness. The strong azimuthal jet manifests itself by the maxima of $\gamma_{\theta f}$ (see Fig 5a). It increases with the Taylor number. The strength of radial jet can be deduced from the axial gradient of γ_{zf}. Its maximum value is also in the forward critical point.

The shear rates and their components were calculated from the measured limiting diffusion currents using the quasi-steady approach, i.e. the Lévêque solution. Taking into account the inertia of the diffusion boundary layer, the amplitudes of oscillations will be even higher.

4. Conclusions

The three-segment ellectrodiffusion probes are convenient for the mapping of the shear rate components on the wall of the wavy Taylor-Couette flow.

The form of the axial distribution of filtered wall shear rate components is similar to the distribution in steady Taylor vortices. However, the maximal values are more important. Jet like outflow characterized by forward critical point was identified. The oscillations of axial component of shear rate exhibit maximum oscillations whereas the oscillations of the azimuthal component are negligible in the forward critical point.

The effect of the inertia of the boundary layer on the oscillation amplitudes should be studied in the future

References

Akonur A., Lueptow R.M., 2003, Three-dimensional velocity field for wavy Taylor-Couette flow, Physics of Fluids, 15, 947-960.

Alekseenko S., Markovich D.M., 1994, Electrodiffusion diagnostics of wall shear stresses in impinging jets, J.Appl. Electrochemistry, 24, 626-631.

Cognet G., 1971, Utilisation de la polarographie pour l'étude de l'écoulement de Couette. J.de Mécanique 10, 65-90.

Coughlin K.T., Marcus P.S., 1992, Modulated waves in Taylor-Couette flow Part 2. Numerical simulation, J. Fluid Mechanics, 234, 19-46.

Jones C.A., 1985, The transition to wavy Taylor vortices, J. Fluid Mechanics, 157, 135-162.

Lebouché M., 1970, Relation entre les fluctuations pariétales du transfert massique et du gradient de vitesse dans le cas d'un nombre de Schmidt grand, Comptes Rendus de l'Académique des Sciences, 271, 438-441.

Lévêque M.A., 1928, Les lois de la transmission de la chaleur par convection, Ann. Mines, 13, 201-239.

Schlichting, H., 1968, Boundary Layer Theory. McGraw-Hill, New York.

Sobolik V., Mitschka P., Menzel T., 1988, Method of manufacture of segmented probe with circular cross-section. Czech Patent. N° 262 823.

Wein O., Sobolik V., 1987, Theory of direction sensitive probes for electrodiffusion measurement of wall velocity gradients. Coll. Czech. Chem. Commun, 52, 2169 - 2180.

Sobolik V., Jirout T., Havlica J., Wall shear rates in Taylor vortex flow. J.Applied Fluid Mechanics, in press.